THESIS

INVESTIGATION OF THE EMISSIVITY OF GRAPHITE WHEN IT IS COATED WITH CADMIUM TELLURIDE (CdTe)

Submitted by

Venkat Anirudh Karteek Gummadala

Department of Mechanical Engineering

In partial fulfillment of the requirements

For the Degree of Master of Science

Colorado State University

Fort Collins, Colorado

Summer 2015

Master's Committee:

Advisor: Walajabad Sampath

Allan Kirkpatrick
James Sites

ABSTRACT

INVESTIGATION OF THE EMISSIVITY OF GRAPHITE WHEN IT IS COATED WITH CADMIUM TELLURIDE (CdTe)

Today, thin film CdTe solar cells are used commercially in many applications. Advances in this technology can aid in meeting increased energy demands. Research is focused on increasing the efficiency of solar cells. By creating more value with minimum environmental impact, Cadmium Telluride (CdTe) solar cells promise to have the potential to become one of the leading eco efficient energy solutions available in the photovoltaic (PV) market today. CdTe PV has been commercialized at the GW/year level.

Many deposition systems for CdTe PV employ graphite structures and they get coated with CdTe during operation. The objective of this thesis is to investigate how the emissivity of the Photovoltaic production tool using graphite surfaces is affected when coated with CdTe at the operating conditions. According to the published literature graphite has an emissivity of 0.65-0.95 and CdTe has an emissivity ranging between 0.2 – 0.8 depending upon the radiation and wavelength range.

The current study was done in three steps. In the first step, the reflection and emissivity of Graphite coated with CdTe was calculated using Kirchhoff's Law of Radiation. In the

second step, graphite-CdTe layer stack was simulated using thin film optical software and reflection data for different thicknesses of CdTe coated graphite was calculated. In the third step, the Advanced Research Deposition system in the Materials Engineering Laboratory was used to deposit CdTe on graphite substrates using a Close Space Sublimation deposition process. The graphite substrates were made from material similar to those used in these applications. The substrates were purified to remove impurities. The CdTe thickness was measured using a Taylor Hobson Profilometer. Rate of heating and cooling of graphite was measured and compared to the rate of cooling of graphite substrates coated with CdTe to evaluate the emissivity.

Results in all the three steps showed that CdTe coating had a negligible effect on the emissivity of graphite at the conditions simulating the production environment.

ACKNOWLEDGEMENTS

I would like to take this opportunity to thank my advisor, Professor Walajabad Sampath, for guiding me throughout my Master`s program. I would also like to thank my committee members, Professor Allan Kirkpatrick and Professor James Sites, for their time and commitment.

I highly appreciate Kevin Cameron for helping me out in various stages of my thesis, especially in explaining the operation of the Advanced Research Deposition system. I also want to thank Jack Clark of Surface Analytics, LLC for his support in helping me using Taylor Hobson Profilometer.

Finally, I would like to thank my family and friends for encouraging me through ups and downs during these years and for always being there for me and for supporting me in whatever I do.

TABLE OF CONTENTS

LIST OF TABLES

LIST OF FIGURES

CHAPTER 1: INTRODUCTION

Today, huge amounts of capital is being invested into Photovoltaic Research and Development primarily focusing on materials used, increasing the solar cell efficiency, lowering the cost of modules, and systems, and henceforth increasing the reliability of the installed components. Research is being done strategically with companies collaborating with universities. Few of the important technologies chosen for research are silicon based technologies and thin film technologies.

1.1 Wafer based Crystalline Silicon Solar Cells

Since the emergence of Solar PV technology, Wafer based crystalline Silicon (Si) solar panels played a major role in the PV market. Huge progress was made (20% decrease in price for each doubling of cumulative installation of capacity), this is due to the expansion of the market and new improved technologies.

Research is focused on issues like decreasing the amount of silicon and other materials used in the module, finding new technologies to manufacture cost effective, high quality of wafer (or equivalent) material and silicon, high yield integrated industrial processing, processing techniques with less environmental impact and increasing the efficiency of modules using some new and integrated concepts.

1.2 Emerging PV Technologies

The research in PV is more or less based on the Crystalline Silicon and thin film technologies. With present research plans the attempts to further reduce the cost per watt produced and increasing the efficiency of these modules beyond 25% looks slim. There is a need for some new emerging and novel technologies. An early detection of an opportunity in the fields of nanotechnology, nanomaterials, photonics, and plastic electronics is needed. By emerging technologies we mean the technologies which already exists and could be considered as a long term option and by novel we mean ideas that could potentially lead to completely newer technologies which can reduce the cost and increase the efficiency although a correct estimate cannot be given.

Emerging PV technologies aim at 15% efficiency at a very low production costs. Technologies considered in this category are Advanced Inorganic Thin-Film Technologies and Organic Solar Cells.

In Organic solar cells, the active layer consists of an organic dye suitable for liquid processing, thus allowing the possibility of printing active layers, thereby boosting production. There are two branches in this technology, hybrid approach and full organic approach, the main goal of these technologies is to increase the efficiency to 10% by 2015.

1.3 Existing thin film technologies

The three major inorganic thin film technologies available in the PV market are amorphous/microcrystalline silicon (TFSi - 13% efficiency), and the polycrystalline semiconductors CdTe (21.5 % efficiency) and CIGSS (an abbreviation of Cu(In,Ga)(S,Se) 2 - 19.5% efficiency). These technologies have a good scope to reduce the cost of manufacturing since they require only a small quantity of source or active materials. Though the present market share of this technology is less than 10%, they have the potential to increase.

Common issues in this technology are

1) Standardizing the product sizes and deposition techniques so that handling would be easy during the deposition

2) New and low cost packaging of the active layers, barrier coatings, polymer foil to reduce material cost and to enhance productivity

3) Better in-line processes for packaging

4) Techniques for mounting and interconnecting the modules

5) Better sealing solutions with good life times during manufacturing

6) Improvement in supply chain logistics for large scale production and quality control methods

7) Finding alternative materials with different band gaps for wide spectrum absorption.

8) Improvement of the quality and stability of transparent conductive oxide (TCO) layers and reducing the cost of TCO is required.

Of the three thin film technologies, CdTe thin film technology offers competitive advantage over the others. The following section elaborates this technology.

1.4 CdTe thin film Solar cell

CdTe used in the thin film solar cell manufacturing has the highest theoretical efficiency over any other material available in the PV market today. Thus holding an edge over other photovoltaic materials available in the market [1].

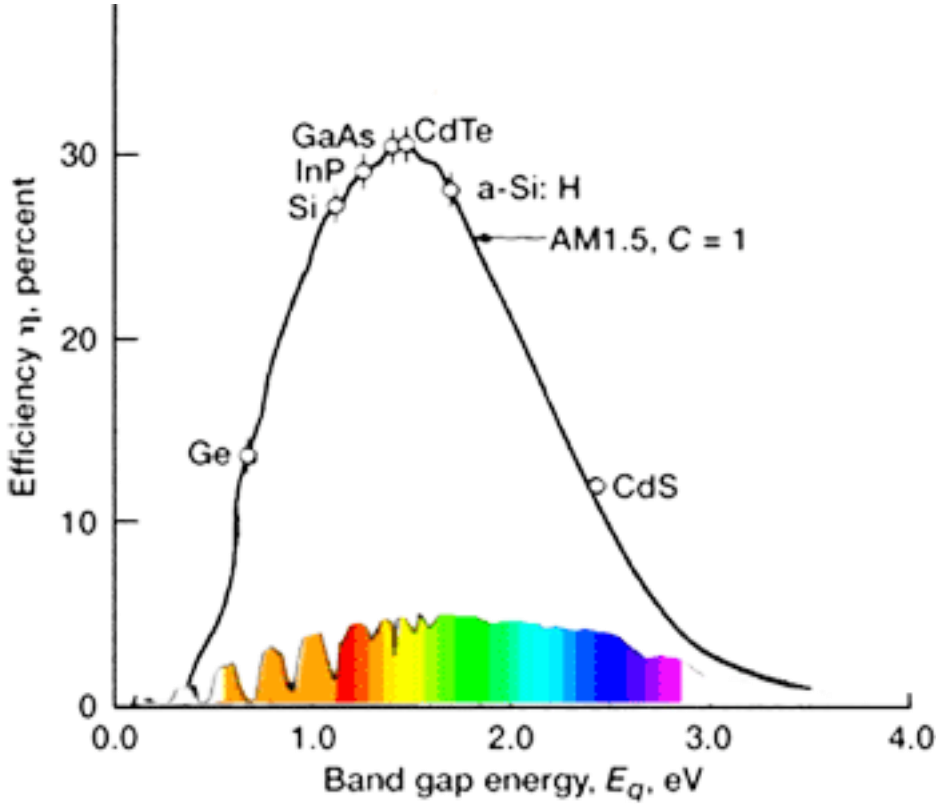

Figure 1: S-Q Curve

The above curve is called the S-Q limit (Shockley-Queisser limit) curve, it explains the efficiency limit for single-junction conversion of the solar spectrum. So far only 21% efficiency has been achieved in research, thus there is a good potential for research to

obtain that proposed theoretical efficiency of 30%. Industries are collaborating with universities for the same.

Compared to the multi-step process used in a Silicon in a Silicon solar cell, CdTe manufacturing is an easy process. Also the price of electricity of CdTe technology based solar panels is 5.7 cents/kWh in the best case, the lowest compared to others. With the smallest carbon footprint, fastest energy payback time, and lowest life cycle water use, CdTe PV creates more value with less environmental effect per kilowatt hour (kWh) produced. Apart from these advantages CdTe has the highest temperature coefficient and spectral response than others, thus having a significant performance advantage compared to conventional crystalline silicon solar modules.

The materials used in the module are sustainably sourced from the industries as the byproducts of the zinc and copper elements.

With all these inherent advantages, once encapsulated in the modules, CdTe produces clean, affordable solar energy for 25 plus year lifetime.

1.5 Current Status of CdTe PV Technology

Currently in US, CdTe photovoltaics (PV) is the leading solar technology that is cost competitive with fossil fuels in many applications [2]. The price of electricity from CdTe PV is currently competitive with electricity produced from the grid in many parts of the world (6 cents/kWhr from utility scale projects) [3] without subsidy and the costs are

decreasing at approximately 7% per year. This compares very favorably with the cost of electricity generation from coal fired power plants and it is nearly half the cost of electricity from gas fired turbines used for generation of peak power [3]. CdTe PV has been commercialized at the GW scale with nearly 10 GW installed. The Aqua Caliente CdTe solar field with 290 MWp installed capacity is shown in Figure 2. This field was completed by First Solar, world leader in PV. Currently CdTe PV is produced by the sublimation process for the semiconductors.

Figure 2: The Aqua Caliente CdTe installation with an installed capacity of 290 MWp

In the materials engineering laboratory with the existing process, devices of efficiency 16.4% have been fabricated on low cost soda lime glass substrates using low cost sublimation process with two minute cycle time in modest vacuum [4]. They represent

some of the highest efficiency demonstrated on these substrates. Electricity generation by CdTe PV has significant environmental benefits, substantial reduction in greenhouse gas (GHG) production, and utilizes renewable resources. The table below shows life cycle analysis conducted by Brookhaven National Laboratory [5]. The CdTe industry has adopted a “cradle to cradle” approach and modules at the end-of-life are accepted by the manufacturer and transported and recycled without charge. It is noted that Cd and Te are the by-products of Cu and Zn mining and are present in the environment. CdTe modules are a better way to sequester Cd and Te. The life cycle analysis of CdTe modules shows that there is less Cd in the encapsulated modules than the amount of cadmium that will be emitted by a coal fired power plant for the same amount of energy produced. It is noted that the Cd in the CdTe modules is sealed between two glass plates whereas the emission from the coal fired power plant is released to the atmosphere. Te is less abundant but in 2007, it was estimated that there is enough known Te to produce terawatt of modules [6]. Since then more sources of Te have been discovered.

Table 1: Pollution prevented by CdTe PV module for each GWh of electricity generated compared with UCTE grid mixture (Insolation = 1700 kWh/m^2/year, lifetime = 30 years) [5]

	Emission reduction	Unit	Percentage
GHG	458	t CO2-eq	95
NOx	0.8	t	95
SO2	1.8	t	97
Arsenic	30	g	97
Cadmium	8.9	g	97
Chromium	74	g	97
Lead	103	g	97
Mercury	13	g	97
Nickel	269	g	97
Thorium-230	8	kBq	98
Uranium-238	35	kBq	98

UCTE= Union for the Co-ordination of Transmission of Electricity, UCTE). The composition of the UCTE is
fossil fuel 50%, nuclear 34%, hydroelectric 15%, and other1%. kBq is kilo Becquerel, GHG is greenhouse gas.

CHAPTER 2: EMISSIVITY OF CdTe FROM LITERATURE

The emissivity of the surface of a material is its effectiveness in emitting energy as thermal radiation. It is one of the factors affecting the thermal performance of a surface. In our current study, we investigated how the emissivity of the photovoltaic production tool using graphite surfaces is affected when coated with CdTe at operating temperatures. From theory, in Transmission vs Wavelength for CdTe, CdTe transmits everything above 1μm, means Emissivity is very low (negligible). While graphite is all absorbing in this range. Hence, when we coat low emissive material on a high emissive material, overall emissivity might change. When literature survey was done it was found that depending upon the radiation and wavelength range considered different values of emissivity for CdTe and graphite are obtained. This chapter presents literature review on the emissivity of CdTe and graphite.

The emissivity of CdTe as a function of temperature, ε (T) can also influence the vapor growth process. The emissivity of CdTe as a function of wavelength and temperature were studied by Mullins [7]. The high temperature optical properties of cadmium telluride have been studied at temperatures up to 1104 K by measurement of the incandescence spectra from a wafer of that material. The experimental set up had quartz ampoule with a highly transmissive and non-emitting optical window. It was found that that emissivity of the sample is a maximum at photon energies where the wafer is expected to be highly absorbing, and falls at lower energy as the sample becomes transmitting. This drop in emissivity shifts to lower photon energies and becomes less

pronounced as the temperature is raised. The slight increases in measured emissivity at approximately 0.79 and 0.90 eV for the highest temperatures of measurement were due to defect related absorption in the quartz window. The emissivity was observed to increase as a function of the temperature, and it was also found that in general the crystal behaved like a grey body rather than a perfect black body. The same study showed the well-known influence of the surface conditions on the emissivity, and suggested its use as a measure of the surface quality and stoichiometry during vapor growth [7].

D C Rodway, M G Astles and D R Wight have studied the effect of the deposition of caesium overlayers on p-type CdTe to check if they can be used in the photoemission devices [8]. A brief study was carried out to determine the suitability of CdTe (Cs) or CdTe (Cs,O) as a possible alternative to GaAs (Cs, O) in photoemission devices. The CdTe layers used in this study were grown by liquid phase epitaxy (LPE) in a conventional graphite horizontally sliding-boat system at atmospheric pressure in a hydrogen ambient. The layers were grown over a temperature range of 500-400 °C at 1 °C/ min cooling rate and were doped with As in the growth solution and were typically 5-6 pm thick. The layers were introduced into the vacuum system either directly from the growth kit or after an etch in bromine/methanol or hot sodium cyanide. Then the samples were heated to radiation from a hot rhenium filament and the temperature was monitored using a pyrometer operating in the 5 microns band. Thermal performance of this system was needed to be evaluated, for this a calibration experiment against thermocouple was conducted and an emissivity value of 0.8 was obtained. The results

in this research showed that it was not possible to produce photoemission devices using CdTe surface by the techniques used for GaAs.

In another study by Zhenjie Chen, Yuming Zhou, Tao Zhang, Xiaohai Bu and Xiaoli Shen on the preparation and characterization of optically active polyacetylene on CdTe quantum dots composites with low infrared emissivity, HPA@CdTe and RPA@CdTe composites were prepared by the surface modification of CdTe quantum dots [9]. Polyacetylene was grafted onto the surfaces of CdTe without destroying the original structure. Initially the values of emissivity for RPA, HPA and CdTe were 0.741, 0.609 and 0.644. Then the infrared emissivity of the composites and the two components was investigated with an IRE-1 Infrared Emissivity Measurement Instrument (shanghai Institute of Technology and Sciences, China). The results showed that emissivity values for composites reduced to 0.342 and 0.424 respectively. The decrease in the value of emissivity is due to the interfacial interactions such as hydrogen bonding or electrostatic interactions between the organic and inorganic components of the composites.
In another instance a Vertical Freezing Growth (VGF) growth setup assisted by axial vibrations of baffle submerged into CdTe melt with controlled Cd partial pressure was designed by few researchers in Russia [10]. An influence of baffle shape on flow velocity map, temperature distribution in CdTe melt and interface shape of growing crystal was analyzed by numerical simulation and physical modeling. The VGF growth setup included cylindrical furnace with 15 one-element zones of resistant plane spiral heaters placed in a groove of thermo conductive (solid Al_2O_3) ceramic ring and with a ring of thermo resistant (porous Al_2O_3) ceramic placed above. A graphite reactor with

CdTe melt and crystal phase, a graphite vibrating rod and a baffle were placed inside the cylinder of heaters. All empty space above the melt and between the walls assumed to be air. Numerical simulation of radiation and conductivity heat transfer in the furnace with fixed uniform temperature gradient in furnace was run on ANSYS Fluent 14.0. All the materials but air were not transparent for the radiation. From the numerical simulation the material properties are found to be air had diffraction coefficient 1, scattering and absorption coefficients are both equal to zero, emissivity of CdTe and graphite were equal to 0.8.

In Transport phenomena in Heat and Mass transfer by J.A. Reizes it was mentioned that CdTe emissivity is equal to 0.2 [11]. It says that CdTe is more like graphite at those conditions. The study of the properties of graphitized carbon materials at high temperatures and pressures for experimental determination of the emissivity of isotropic graphite at temperatures above 2300K was done by A. V. Kostanovski, M. G. Zeodinov, and M. E. Kostanovskaya. The experimentally obtained values of monochromatic normal emissivity for Grade MPG-7 isotropic graphite depending on the temperature are found to be varying between 0.83-0.89 in the temperature range of 2100K- 3200K. In the region of temperatures of 3200–3600 K, the experiment shows a pronounced decrease in emissivity value (10–15%) in comparison to the values obtained in the temperature range of 2100-3200K. The observed decrease in emissivity may be caused by various reasons. One of the possible reasons may be a process which defines a spontaneous increase in temperature. The literature on emissivity of CdTe and graphite are summarized below in Table 2.

Table 2: Emissivity values for CdTe from Literature

Material	Emissivity	Single/Polycrystalline	Temp(°C/K)	Wavelength	References
1)CdTe	0.6-0.8	Poly	827-1104K	0.6-1.8µm	J. T. Mullins, J. Carles and A. W. Brinkman. "High Temperature Optical 5Properties of Cadmium Telluride ". J. Appl. Phys., 81 (1997) 6374
2)CdTe	0.644	Poly	Room Temp	8-14µm	Zhenjie Chen et al., Preparation and Characterization of Optically Active Polyacetylene@CdTe Quantum Dots Composites with Low Infrared Emissivity. Journal of Inorganic and Organometallic Polymers and Materials May 2014, Volume 24, Issue 3, pp 591-599
3)CdTe	0.6	Poly	1365k	N/A	CdTe crystal growth process by the Bridgman method:Numerical Simulation
4)CdT	0.7	Poly	525	N/A	High emissivity distribution plate in

e					vapor deposition apparatus and processes by Mark Jeffrery Pavol and christopher Rathweg
5)CdTe	0.2	Poly	1392-892K	N/A	Thermal Stresses Near the Crystal-Melt Interface During the Floating-Zone Growth of CdTe Under Microgravity EnvironmentLee Kyu-Jung ;Journal of computational fluids engineering, volume 3, issue 1, 1998, Pages 100-107
6)CdTe	0.7	Poly	310°C	N/A	Selective growth of CdTe on patterned CdTe/Si by T. Seldrum, R. Bommena, L. Samain, J. Dumont, S. Sivananthan andR. Sporken
7)CdTe	0.8	Poly	400-500°C	Normal room conditions	D C Rodway et al., 1983. In situ AES and work-function study of the deposition of caesium on CdTe. Journal of Physics, D: Appl.

					Phys. 16 2317, 1983

Table 3: Emissivity values for Graphite from Literature

Material	Emissivity	Temp °C/K	Wavelength	References
1)Graphite	0.83-0.9	2200-3200K	0.65µm	The study of the properties of graphitized carbon materials at high temperatures and pressures for experimental determination of the emissivity of isotropic graphite at temperatures above 2300K by A. V. Kostanovski, M. G. Zeodinov, and M. E. Kostanovskaya
2)Graphite	0.72-0.81	>3200k	0.65µm	properties of graphitized carbon materials by M. G. Zeodinov

3)Graphite	0.78	1285-2035	N/A	A black-body source of radiation covering a wavelength range from the ultraviolet to the infrared. K C Lapworth, T J Quinn and L A Allnutt
4)Graphite	0.75-0.9	1600-2150K	0.65µm	A black-body source of radiation covering a wavelength range from the ultraviolet to the infrared. K C Lapworth, T J Quinn and L A Allnutt
5)Graphite	0.75	300°C	N/A	High emissivity distribution plate in vapor deposition apparatus and processes by Mark Jeffrery Pavol and christopher Rathweg

CHAPTER 3: CdTe THIN FILM SOLAR CELL MANUFACTURING

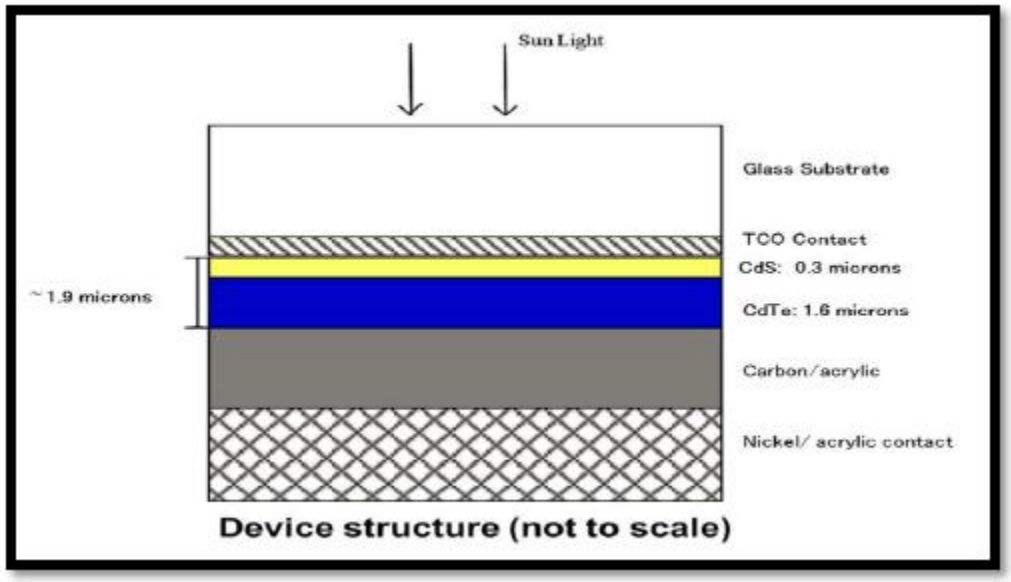

Figure 3: CdTe Schematic Device Structure (Not to scale)

Basically a CdS/CdTe solar cell is made up of a glass substrate, transparent conducting oxide layer (TCO), n- type CdS semiconductor layer and p-type CdTe semiconductor layer and Carbon Nickel acrylic back contact.

The manufacturing process of CdS/CdTe solar cells involves thermal sublimation. The operation of such process is carried out in a vacuum environment. Many stages and sub processes are part of this manufacturing process, hence necessary care is taken to maintain a highly controlled atmosphere, environmental conditions, temperature and pressure. The glass substrates coated with TCO are obtained from commercial sources. These substrate are cleaned ultrasonically with isopropyl alcohol and dried in a clean room environment. This substrate with TCO coating on one side and soda lime on the

other is transported into vacuum chamber where it is heated to a temperature range of 500-600°C. The depositions of CdS and CdTe are subsequently made on the substrate and these layers are treated with $CdCl_2$ (Cadmium chloride) at a reduced temperature (300-500°C) to increase the efficiency of cell. Later, $CdCl_2$ is removed from the stack through annealing process and the layers are cooled to a temperature range between 20-100°C and taken to an ambient atmosphere. A small amount of copper is introduced into the back of CdTe by the sublimation of CuCl and annealing. The CdTe is contacted with graphite particles and nickel particles in acrylic binder.

CHAPTER 4: EQUIPMENT DESCRIPTION

In the current study, in the third part of our work we used the Advanced Research Deposition System (ARDS) to deposit the CdTe film on the four different graphite substrates, Taylor Hobson profilometer to measure the respective film thicknesses on those substrates and Pyrometer to measure the rate of cooling of graphite substrates. This chapter briefly discusses the description and the working principles of these equipments.

4.1 Advanced Research Deposition System (ARDS)

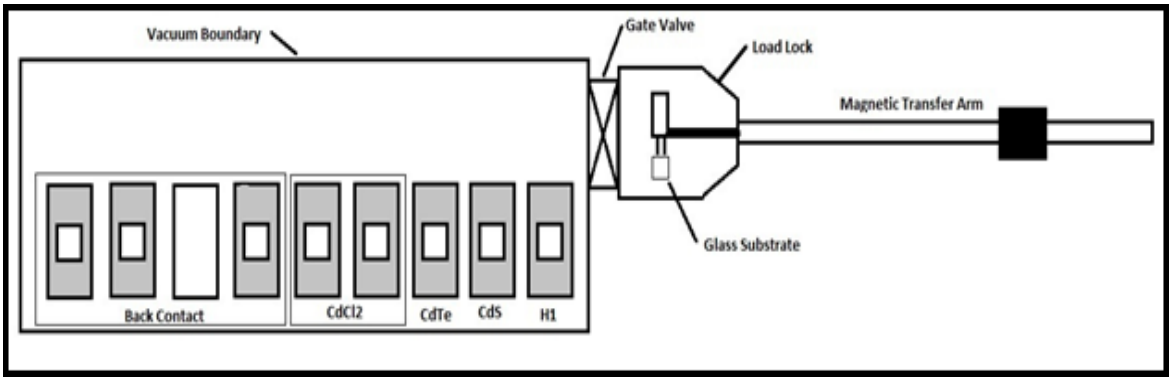

Figure 4: Schematic of the Advanced Deposition System (ARDS)

The process chamber used for the experiment is the Advanced Research Deposition System (ARDS) located at the Colorado State University's Engineering Research Center.

The ARDS uses Close Space Sublimation (CSS) as the deposition process. In the ARDS, the heating of the graphite sources is done with ceramic potted Nichrome (NiCr)

heaters which induce sublimation of the source's material followed by vapor condensation onto the substrate. The substrate sits on an end effector approximately 1.25 mm off the top of the source pocket.

The substrates are manipulated to each of the nine stations as programed using an automated transfer arm manufactured by Transfer Engineering and Manufacturing, Inc. out of Fremont, California. The ARDS incorporates a plasma cleaning system located on the load lock which is a secondary pre-cleaner for the glass substrates. The ARDS has the capability to measure substrate temperatures through the use of a pyrometer and also utilizes a residual gas analyzer (RGA) to measure partial pressures of gases present in the system.

The ARDS is a versatile process tool allowing researchers to change many variables in their research to increase efficiency of CdTe PV devices. During this experiment for the effect of CdTe on graphite emissivity, we utilized position one which is a preheater, position four which deposits CdTe and the position one pyrometer for temperature measurement.

ARDS Process

4.1.1 Chamber set up

Before starting the experiment, the chamber has to be brought to process condition. For the experiment, this required bringing the RGA online to monitor gasses in the

system, heating the sources for sublimation of CdTe, valving in the proper process gasses, setting the process chamber pressure and programing the transfer arm to run the substrate through the required sources. All process runs are archived so the proper data sheets are filled out for data storage along with the RGA graphs and any other data the tool operator deems relevant.

To run this experiment, the process tool was set up as follows:

1)The RGA was turned on and valved into the system.

2)The process gas was valved into the system consisting of 2% Oxygen with a balance of UHP(Ultra High Purity) Nitrogen.

3)The position one heaters were brought up to 620^0C and the CdTe top heater was brought to 360^0C while the bottom heater/source was brought to 554^0C.

4)All other system heaters were brought to what is referred to as “idle” temperatures. This is a temperature at which the heaters are ramped to a set point as hot as possible without sublimating the contained material.

5)The transfer arm was programed to run the graphite substrate into the position one preheater and the CdTe sublimation source.

Figure 5: Figure showing the ARDS setup

4.1.2 Process Operations

Normally, for the glass substrates typically run through the ARDS, there is a whole cleaning process utilizing alcohol, liquid detergents and DI (Deionized water) water. However, due to the porosity of graphite, using a liquid cleaning process was not an option. The graphite substrates were simply blown off with Argon gas and wiped off using a cleanroom wipe called Kim wipes prior to deposition. Latex gloves were used at all times while handling the graphite substrates.

To load the graphite substrates, the procedure followed is described below

1) Ensure the gate valve is closed isolating the load lock from the process chamber.

2) Vent the load lock to atmosphere using N2 (Gaseous Nitrogen).

3) Load graphite substrate on end effector making sure it is securely in place.

4) Open the load lock fore line valve to pump down the load lock to < the process chamber pressure.

5) Close the load lock fore line valve and open the gate valve to the process chamber.

6) After verifying proper heater temps and chamber pressure, the experiment is started.

After the use of ARDS experiment to coat the CdTe film on the four graphite substrates we use the Taylor Hobson Profilometer to measure the individual film thicknesses.

4.2 Taylor Hobson Profilometer

Taylor Hobson Form Talysurf PGI 1230 was used to determine the individual film thicknesses of CdTe deposited on the four graphite substrates. Form Talysurf PGI 1230 is specially configured for super precision bearings of all sizes. Basic configuration of this system has 200mm traverse with 0.125μm straightness uncertainty, 450mm column and 12.5mm gauge range with 0.8nm resolution. In order to avoid or reduce the air movement and to escape from contamination, an environmental isolation chamber is located.

Figure 6: figure showing the measuring station of Taylor Hobson Profilometer

4.2.1 Measuring station

Both the column and the base are made of composite granite material to provide high vibration dampening, thermal inertia and stiffness throughout the measuring loop. It has a massive base that isolates the instrument from vibration and offers plenty of room for staging large components. Two tee slots, parallel to each other within 0.3mm (0.01in),are provided for precise mounting of accessories. The equipment has a column that is fully motorized to do vertical and tilting movements for programmability and total automation. It has

•A servo controlled motor driver and an encoder for up/down movements. The maximum positioning speed is 10mm/second (0.4in/second).

• Allows tilt control (+/- 9º range), thus making life easy for traverse unit to be automatically adjusted parallel to inclined surfaces

•Automatically advances the stylus to the workpiece and stops on contact centered in the middle of the gauge range

It also has welded steel frame, which rigidly supports the base and motorized column.

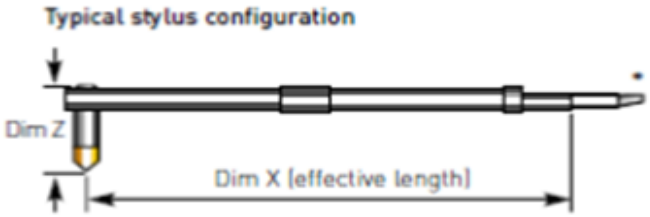

Figure 7: figure showing stylus configuration for Taylor Hobson Profilometer

In our equipment, Stylus force change is less than 5% and improved stylus arm mounting design offers easy interchangeability along with absolute rigidity. The standard coarse for our stylus arm has Dim X 60mm, Dim Z 8.3mm, Tip angle 90 degrees, Tip radius 5microns.

The digital Surf's software was used in the study to fit a least square line to measure the film thickness. This software is compatible with Taylor Hobson profilometer and the software was used for analyzing surface geometry, surface texture and for calculating related parameters according to the ISO and ASME standards. The software allows studying roughness profiles, waviness profiles of a sample independently and also

studying the relationships between two profiles by superimposing one over another. In our study, the step analysis reports were carefully studied using available templates and the results were obtained.

4.3 Pyrometer

Mikron's M1-N5+ Pyrometer was used for our study. It is suitable for measuring the temperature of objects with non - metallic surfaces (including varnished, oxidized and anodized metals) with a temperature range of -32 to 900°C) and glass surfaces with a temperature range of 100 to 2500°C. It has a stainless steel housing, readings are unaffected by the relative humidity or the amount of CO2 in the air.

The pyrometer operates passively. It receives heat radiation, from the measured object, which passes through the lens and is then converted to an electrical signal. The measured object may be at any distance from the pyrometer. However, the farther the measured object is from the pyrometer, the larger the area that will be measured by the pyrometer.

An integrated microprocessor performs all calculations and digital signal processing. Together, with the signal from the ambient temperature compensation feature, it optimizes the accuracy of the measurement by compensating for the effects of reflected ambient energy. The pyrometer is supplied with either an RS 232 or RS485 serial interface. All setup parameters are remotely adjusted via the digital interface using Mikron InfraWin software.

For precise aiming and alignment of the pyrometer, an optional laser targeting is available. The laser dot indicates the exact center of the circular measurement area and can also be left ON during measurements.

The controls/switches are located under the rear cover of the pyrometer and can be accessed by removing the rear cover. To remove the rear cover we unscrewed both the rear screws and take the cover off, making sure it remains straight (without bending or twisting it). Then while reassembling it we carefully insert it into the guide pins and then fasten it with the screws.

The pyrometer is powered by 24V DC +/- 25%. We need to check for polarity while connecting to the device. The device does not need to be warmed up or run in advance and can be made to use immediately.

A shielded connecting cable is used to meet the electromagnetic requirements. The shield of the two wire connecting cable should only be connected on the pyrometer side. If the connecting cable is extended, the extension cable also needed to be shielded. We do not connect the shield to the power source side to avoid ground loops.

The response time t90 which is the time taken to reach 90% of the recorded temperature difference is measured as the time interval from the start of measurement up to the respective change in the output signal (4-20mA). When the 4 DIP switches (t90= 0.5s, 1s, 2s and 5s) are in the OFF position, the device operates using the time

constant 0.08 sec. The DIP switches are used to set the response time. The pyrometer is equipped with water cooling jacket with integrated air purge. It protects the pyrometer in extremely hot ambient temperatures. It is completely closed and is equipped with a long air purge tube to protect the lens. With this heavy duty cooling jacket, the pyrometer may be operated at ambient temperatures up to 280°C when using a cooling water temperature of 14°C and a cooling water flow rate of 2l/min. Maximum water pressure is 10bar.

In the present study the pyrometer was used to determine the values of rate of cooling for both plain and coated graphite substrates.

CHAPETR 5: THEORETICAL CALCULATIONS

5.1 Kirchhoff's Law of thermal Radiation

In the first part of our study, we used of Kirchhoff's law of thermal radiation. In thermodynamics, Kirchhoff's law of thermal radiation refers to a material in thermal equilibrium that is wavelength-specific, emitting and absorbing electromagnetic radiation.

The dimensionless coefficient of absorption is the fraction of incident light that is absorbed by the material when it is radiating and absorbing in thermal equilibrium. In alternative terms, the emissive power of a body of certain size and shape at a particular temperature can be best described by a dimensionless ratio, emissivity, which is the ratio of the emissive power of the body to the emissive power of a black body of the same size and shape at the same fixed temperature. From this definition, a proposition that can be made of Kirchhoff's law is that for a body of any arbitrary material emitting and absorbing thermal radiation in thermodynamic equilibrium, the emissivity is equal to the absorptivity.

$\epsilon = \alpha$

Where, ϵ is emissivity and α is absorptivity.

If the amounts of radiation energy absorbed, reflected, and transmitted when radiation strikes a surface are measured in percentage of the total energy in the incident electromagnetic waves. The total energy would be divided into three groups, they are

called absorptivity (α), reflectivity (ρ) and transmissivity (t) and they can be put into a equation as

$$\alpha + \rho + t = 1$$

Where,

Absorption is the fraction of irradiation absorbed by a surface

Reflectivity is the fraction reflected by the surface

Transmissivity is the fraction transmitted by the surface

In the present study, the body being opaque does not transmit any radiation falling on its surface. It reflects a part of it and other part is absorbed. As a result we have

$$\alpha + \rho = 1$$

This again can be put as

$$\epsilon + \rho = 1$$

From literature, the emissivity of graphite is 0.8 (was chosen as the average value), plugging in this value in the above equation we get reflectivity ρ as 0.2.

In the production tool, when vapors of CdTe get coated on graphite, there is a reflection taking place at graphite-CdTe interface and CdTe-Air interface. The amount of light (or radiation) that is reflected can be determined by the reflectivity at that surface. The reflectivity can be calculated from the refractive index and the incidence angle with the Fresnel equations.

Refractive index gives the measure of how light or any other radiation propagates through a particular medium. It is defined as,

$$n = \frac{c}{v}$$

Where *c* is the speed of light in vacuum and *v* is the speed of light in the substance. The Fresnel equations (or Fresnel conditions), describe the behavior of light or radiation when moving between media of differing refractive indices. They also describe the phase shift of the reflected light. The reflections of light that the equations predict is known as Fresnel reflection.

Here, when the radiation moves from a medium of a certain refractive index n1, into a second medium with refractive index n*2,* the reflectance at an interface can be calculated as

$$\mathrm{R1} = (\mathrm{n1} - \mathrm{n2}) \wedge 2 \div (\mathrm{n1} + \mathrm{n2}) \wedge 2$$

Where,

R1 is the reflection at CdTe-graphite interface

n1 is the refractive index of graphite

n2 is the refractive index of CdTe

And

$$\mathrm{R2} = (\mathrm{n2} - \mathrm{n3}) \wedge 2 \div (\mathrm{n2} + \mathrm{n3}) \wedge 2$$

Where,

R2 is the reflection at CdTe-Air interface

n2 is the refractive index of CdTe

n3 is the refractive index of Air

The value of refractive index for graphite can found by considering the reflection at graphite-Air interface. Refractive index of Air is 1.

$$\mathrm{R} = (\mathrm{n1} - \mathrm{n3}) \wedge 2 \div (\mathrm{n1} + \mathrm{n3}) \wedge 2$$

$$0.2 = (\mathrm{n1} - 1) \wedge 2 \div (\mathrm{n1} + 1) \wedge 2$$

$n1 = 2.57$, this matched the value in the literature

Now, plugging in the values of refractive indices of graphite (2.57), CdTe (2.69) [20] and air (1) in the respective equations, we calculated the reflection at both the interfaces. Now, the emissivity of graphite coated with CdTe can be calculated as

$$\epsilon = 1 - (\text{reflection at graphite} - \text{CdTe interface}) - (\text{reflection at CdTe} - \text{Air interface})$$

$$\epsilon = 1 - 0.0005 - 0.21$$

$$\epsilon = 0.79$$

This is equal to the emissivity of plain graphite.

From the above calculations we see that there is no considerable effect on the emissivity of graphite when it is coated with CdTe. CdTe behaved like a transparent agent and the entire radiation was going through the CdTe into the plain graphite. For more accurate calculations, the complex refractive indexes of the materials need to be used and this was done with the thin film optical software described next.

CHAPTER 6: SIMULATIONS USING THIN FILM PROBE SOFTWARE

In the second part of the study, the layer stack of graphite and CdTe was simulated and the reflection data was calculated for different thicknesses of CdTe coated graphite. The licensed software was part of the reflectometer purchased from the company Angstrom Sun Technologies.

6.1 Tf probe software

Optical method is the best approach to characterize the properties of a sample for Reflection, transmission spectra and also individual film or layer properties such as Film thickness, roughness, interface and possibly optical properties themselves. There are different optical techniques like spectroscopic ellipsometry and photometry. Photometry techniques including reflection or transmission measurement are relatively easy to use.

Tf probe software is mainly used for data acquisition for reflection and transmission and film thickness measurement with reflection and transmission data. The software has got a large database of optical constants of materials which can used to establish a layer stack for thickness and reflection measurement, we can also run simulation on reflection with such a stack.

6.2 Operation Procedure

The Thin Film Probe products are designed to determine thin-film characteristics with either reflectometry or ellipsometry or both. The software's inbuilt features use different concepts like wave propagation and polarization, Fresnel's equations, refractive indices to determine the reflection values of the simulated layer stack.

The property by virtue of which electromagnetic waves oscillate in more than one orientations is known as Polarization. Though for a wave, both the electric and magnetic fields are oscillating in different directions, we refer to polarization of electric field as the polarization of light. When this incident light is polarized with its electric field perpendicular to the plane containing the incident, reflected, and refracted rays, the light is said to s-polarized and when the incident light is polarized with its electric field parallel to the plane such light is described as p-polarized.

In the present study, when the radiation strikes the layer stack surface, chances are there that reflection and transmission of light source to take place. The software uses the Fresnel's equations to calculate the respective reflection and transmission coefficient at those interfaces.

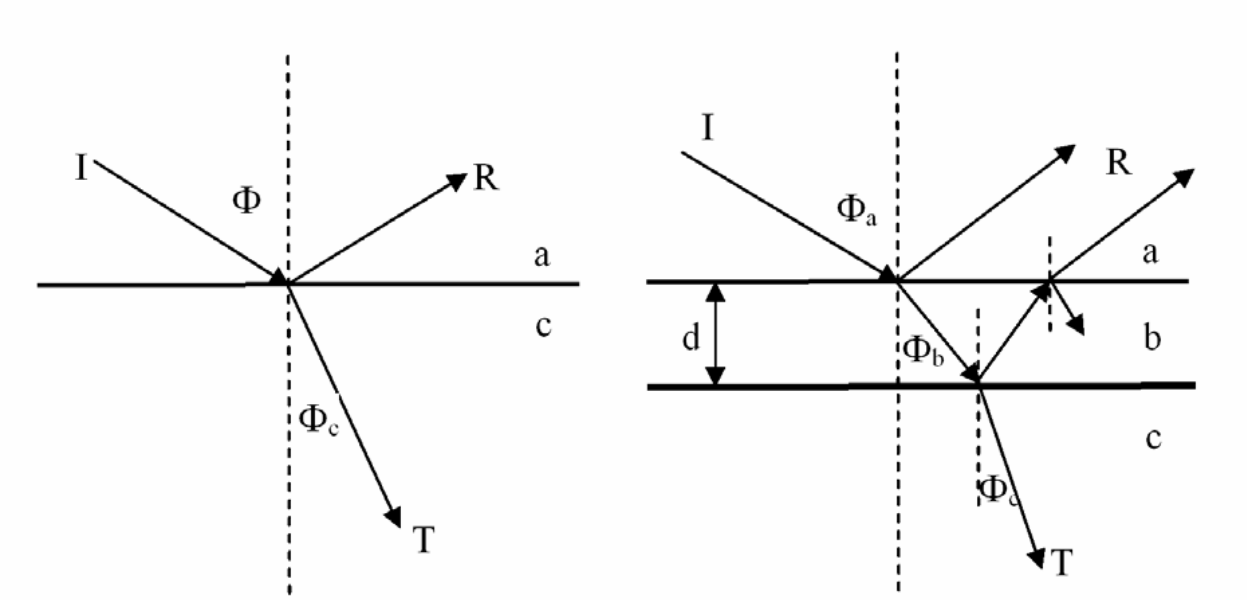

Figure 8: Reflection and transmission of plane wave at two media (a-b) and three media (a-b-c)

Here,

Media c is assumed as semi-infinite absorbing substrate

I is the incident beam

R is the reflected beam

T is the transmitted beam

Using Fresnel's equations, the reflection coefficient at the interface a-c can be calculated as

$$r_{ac}^{P} = \frac{\tilde{N}_c Cos\Phi_a - \tilde{N}_a Cos\Phi_c}{\tilde{N}_c Cos\Phi_a + \tilde{N}_a Cos\Phi_c}$$

$$r_{ac}^{S} = \frac{\tilde{N}_a Cos\Phi_a - \tilde{N}_c Cos\Phi_c}{\tilde{N}_a Cos\Phi_a + \tilde{N}_c Cos\Phi_c}$$

here, superscripts represent p-polarization and s-polarization respectively. r is Fresnel reflection coefficient. Subscripts represent materials in the system. a is media, c is substrate. N is complex refractive index which has following expression

$$\tilde{N} = n - jk$$

n is the refractive index and k is extinction coefficient.

The values of refractive index and extinction coefficient of CdTe in this calculation were taken from the database of the software. The software assigns the respective values depending upon the wavelength considered.

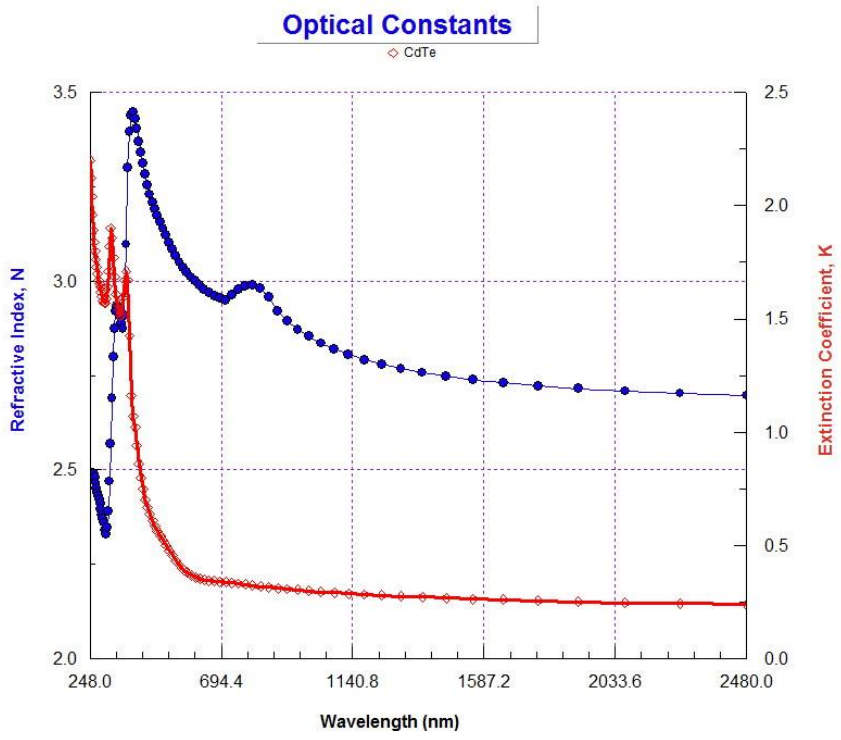

Figure 9: Graph showing optical constants values at different wavelength for CdTe

The refractive index n and extinction coefficient k of CdTe films deposited at CSU was determined from the ellipsometer and the results can be seen in fugures 9-12. It can be seen that the n and k values of CdTe films depend on processing conditions.

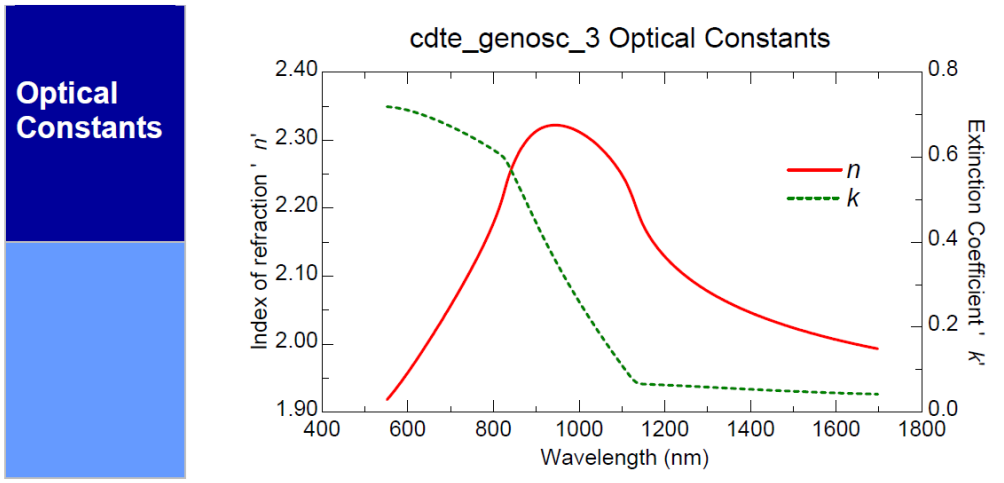

Figure 10: CdTe as deposited on glass with TCO

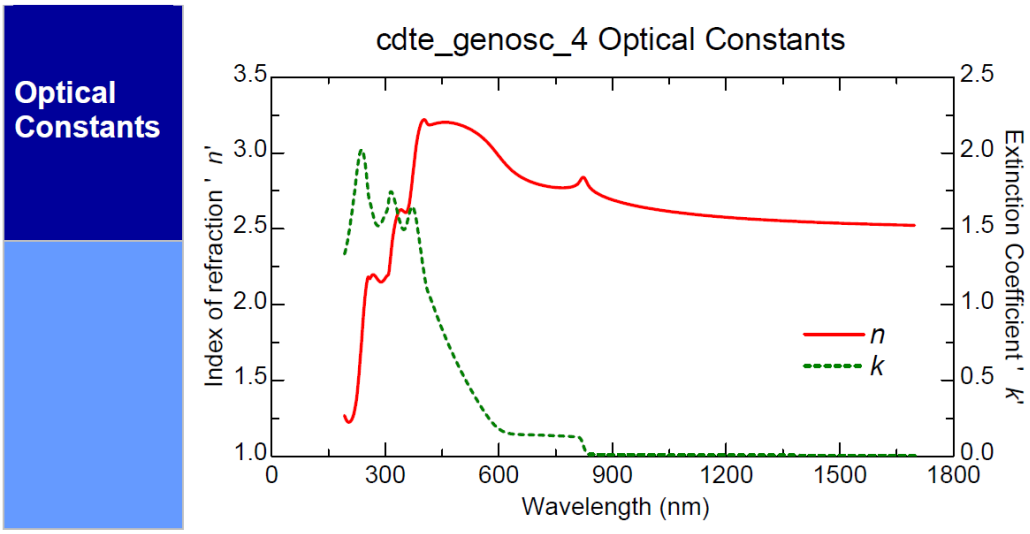

Figure 11: CdTe as deposited + $CdCl_2$ treated + Cu

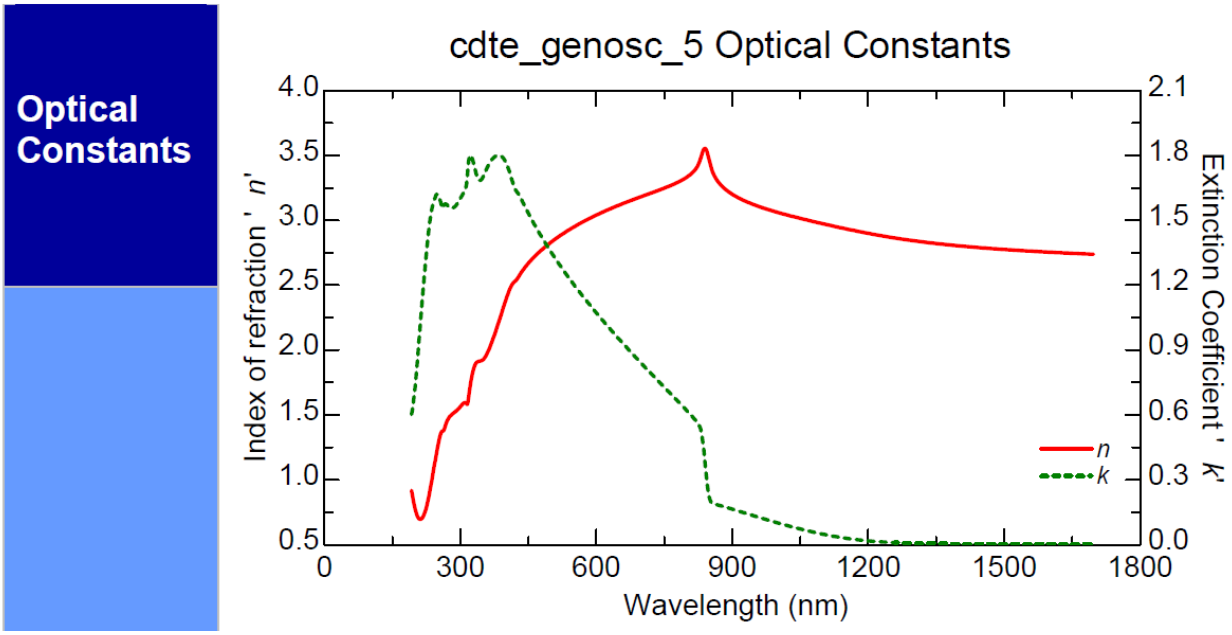

Figure 12: CdTe as deposited + $CdCl_2$ treated

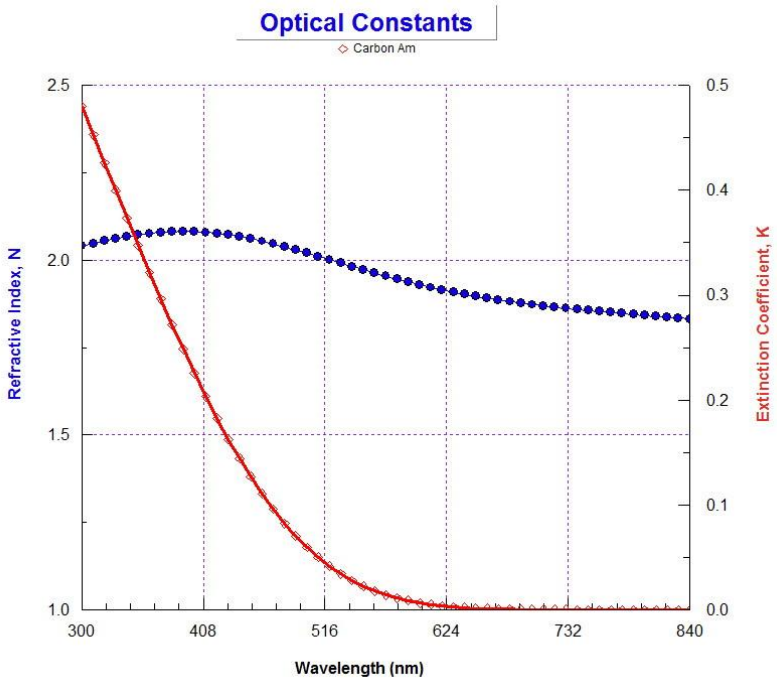

Figure 13: Graph showing optical constants values at different wavelength for Amorphous Carbon

No concrete data was available for n and k of graphite for specific wavelength range and temperatures as they depend on the particle size, manufacturing process, orientation and other conditions

Hence, in this second part of the work using Thin film Optical Software, n and k values of amorphous carbon was shown (as it was the closest available material with respect to graphite in the database of the software), but in reality it is very much different from graphite.

In addition, Φ is the beam incident angle. Its subscripts define the incident angle in which media. The refracted incident angles inside different media can be related to each other with Snell's law:

$$\tilde{N}_a Sin\Phi_a = \tilde{N}_c Sin\Phi_c$$

the transmission coefficient at the interface a-c can be calculated as

$$t_{ac}^{P} = \frac{2\tilde{N}_a Cos\Phi_a}{\tilde{N}_c Cos\Phi_a + \tilde{N}_a Cos\Phi_c}$$

$$t_{ac}^{S} = \frac{2\tilde{N}_c Cos\Phi_c}{\tilde{N}_a Cos\Phi_a + \tilde{N}_c Cos\Phi_c}$$

Where t represents Fresnel transmission coefficients

The total reflection coefficient for three media (a-b-c) system

$$R^P = \frac{r_{ab}^P + r_{bc}^P e^{-j2\beta}}{1 + r_{ab}^P r_{bc}^P e^{-j2\beta}}$$

$$R^S = \frac{r_{ab}^S + r_{bc}^S e^{-j2\beta}}{1 + r_{ab}^S r_{bc}^S e^{-j2\beta}}$$

$$\beta = 2\pi(\frac{d}{\lambda})\tilde{N}_b Cos\Phi_b$$

where R represents total Fresnel reflection coefficients. The β is Phase factor which is generated by existing layer and affected by the layer thickness and optical properties.

From matrix theory of multi-layer systems, if there is a multilayer structure, consisting of m plane-parallel layers sandwiched between semi-infinite ambient and substrate media (0 and m + 1, respectively). The relationships between the field amplitudes of the incident (i), reflected (r), and transmitted (t) plane waves for the p or s polarizations are determined by the scattering matrix equation

$$\begin{bmatrix} E_i \\ E_r \end{bmatrix} = \begin{bmatrix} S_{11} & S_{12} \\ S_{21} & S_{22} \end{bmatrix} \begin{bmatrix} E_t \\ 0 \end{bmatrix}$$

The complex-amplitude reflection and transmission coefficients of the entire structure are given by

$$R = \frac{S_{21}}{S_{11}}$$

$$T = \frac{1}{S_{11}}$$

However, above two are complex expressions. The reflectance and transmittance take the real part of product of above expression with their conjugates.

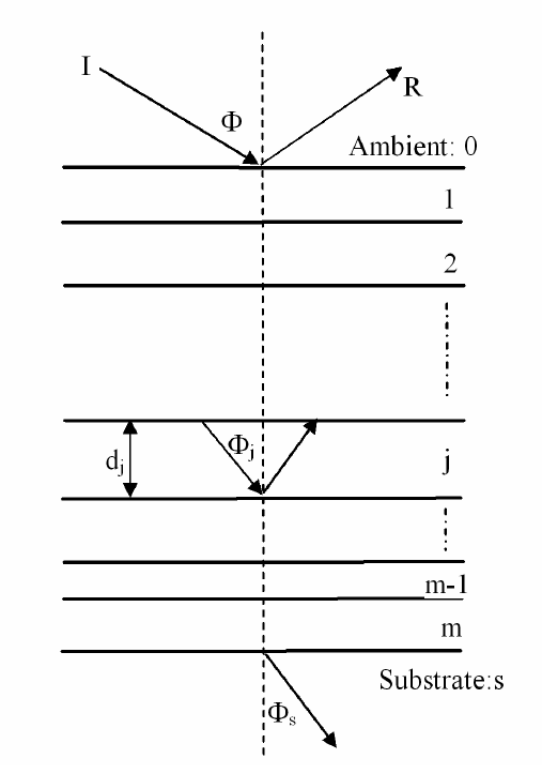

Figure 14: schematic for multi layer stack
The scattering matrix S =(S) ij is obtained as an ordered product of all the interface I and layer L matrices of the stratified structure,

$$S = I_{01} L_1 I_{12} L_2 I_{23} L_3 I_{34} L_4 \ldots I_{(m-1)m} L_m I_{m(m+1)} = \begin{bmatrix} S_{11} & S_{12} \\ S_{21} & S_{22} \end{bmatrix}$$

and the numbering starts from layer 1 (in contact with the ambient) to layer m (adjacent to the substrate) as shown in above figure. The interface scattering matrix is of the form

Interface characteristic matrix I for (a and b):

$$I_{ab} = \begin{bmatrix} 1/t_{ab} & r_{ab}/t_{ab} \\ r_{ab}/t_{ab} & 1/t_{ab} \end{bmatrix} = (1/t_{ab}) \begin{bmatrix} 1 & r_{ab} \\ r_{ab} & 1 \end{bmatrix}$$

Characteristic Matrix L for a Layer:

$$L = \begin{bmatrix} e^{j\beta} & 0 \\ 0 & e^{j\beta} \end{bmatrix}$$

In all the above equations, the values of refractive indices of media, extinction coefficients and other optical properties are taken from the already existing database of materials in the software. The optical values are based on the effective wavelength range considered.

Thus, making use of the above equations the software calculates the reflection at the layer stack interface (graphite-CdTe in the present case).

6.3 Results

The thin film modelling software uses n (refractive index) and k (extinction coefficient) of the different materials to calculate the reflection from the stack. The stack had CdTe with various thicknesses. Thus, after simulating the layer stack of CdTe-graphite with

the help of materials in the database, we calculated the reflection data for four different thicknesses of CdTe coated graphite substrate (graphite was assumed to be thick). Simulation was run on four layer stacks of graphite coated with 1µ, 2µ, 5µ and 10µ of CdTe respectively.

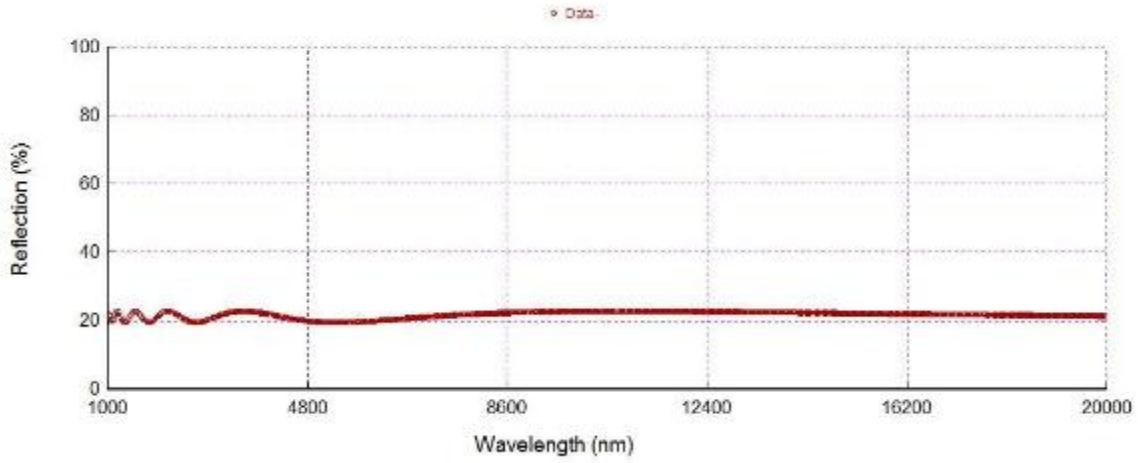

Figure 15: Graph showing reflectance data for graphite substrate coated with 1µ of CdTe

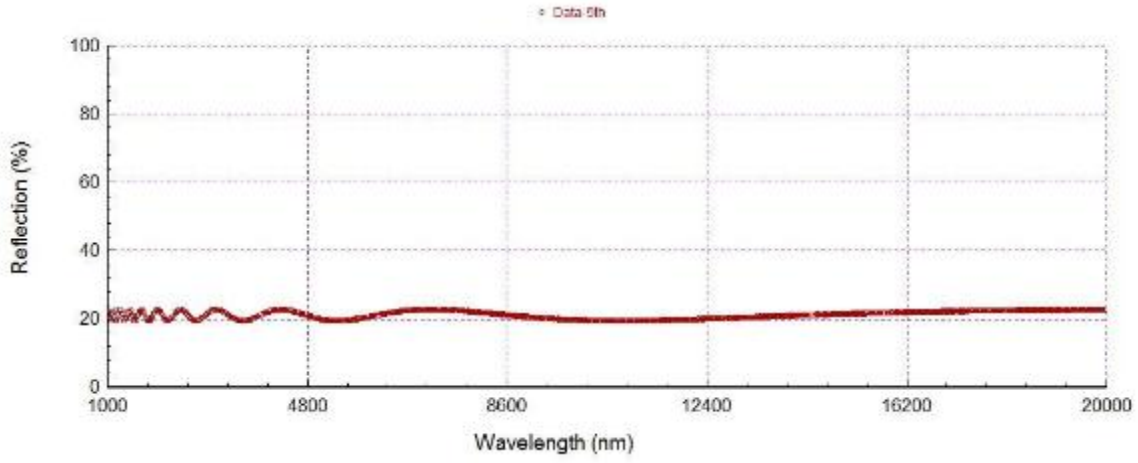

Figure 16: Graph showing reflectance data for graphite substrate coated with 2µ of CdTe

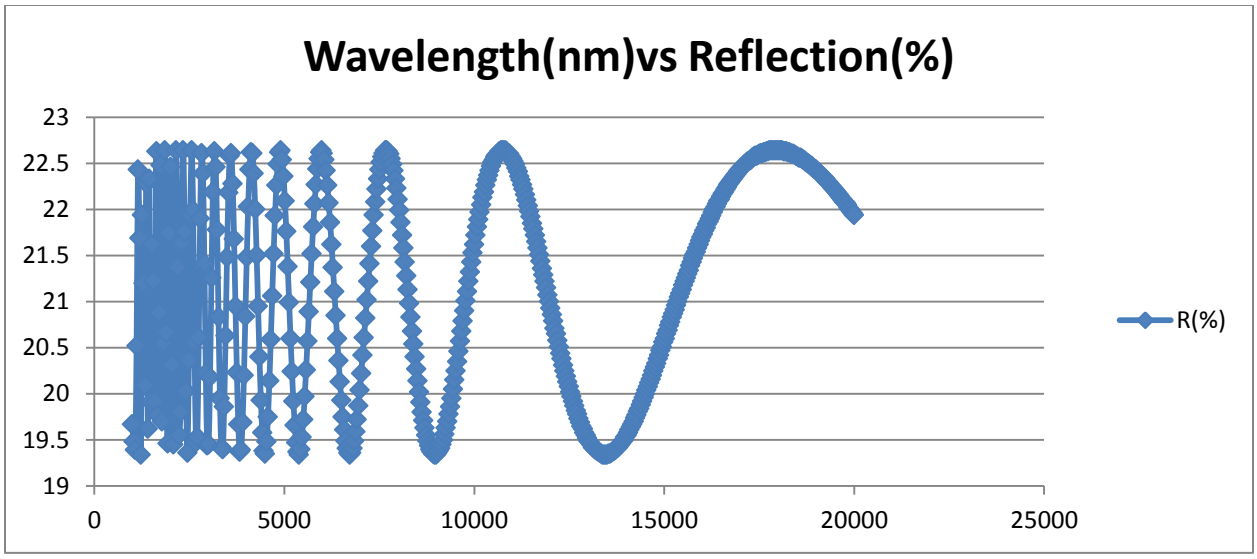

Figure 17: Graph showing reflectance data for graphite substrate coated with 5µ of CdTe

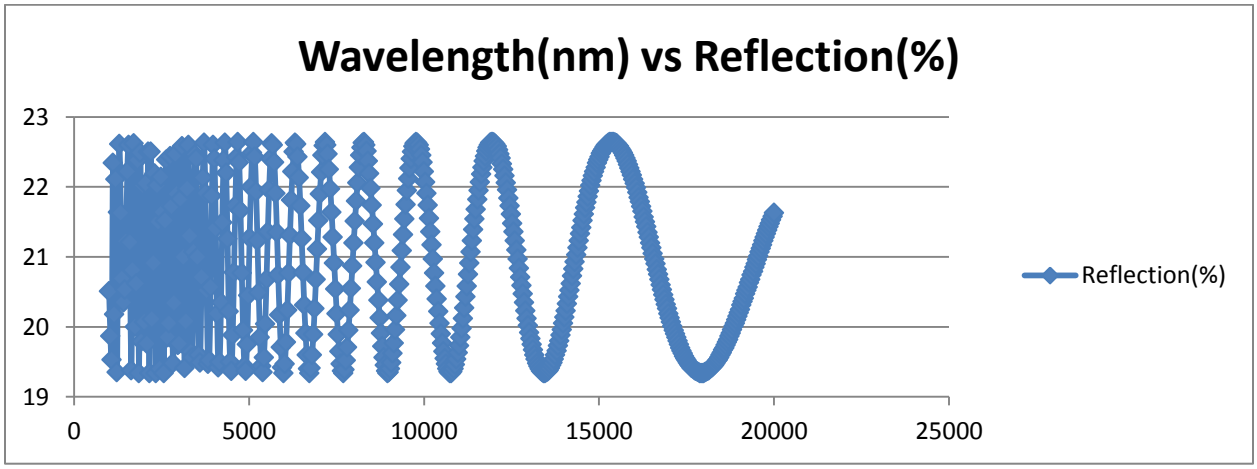

Figure 18: figure showing reflectance data for graphite substrate coated with 10µ of CdTe

The reflection values in all the cases fell in the range of 17-21%. Using the above data we can calculate the emissivity as

$$\epsilon = 1 - (\text{reflection})$$

which gives us the emissivity values falling in the range of 0.79 - 0.83

This exactly matches the previous result of reflectance percentage we deduced using Kirchhoff's law. Thus supporting the previous statement of CdTe having negligible effect on graphite.

Though the calculations in chapter 5 and chapter 6 show no influence of CdTe on graphite, these results cannot be taken as final since we assumed commonly used values for graphite and CdTe from the literature. The emissivity values for both the materials are scattered for different temperature and wavelength ranges, exact numbers were not available. Hence experimental verification was needed.

CHAPTER 7: EXPERIMENTAL VERIFICATION

The results obtained from calculations (previous sections) were verified experimentally. The experimental verification was done at high a temperature (approximately 350°C) which is closer to the industrial operation.

7.1 Experimental Substrates

Five G330 graphite substrates were ordered from Electro-Tech Machining located in Long Beach, California. The Dimensions of the graphite was cut to match the glass substrates typically run in this process tool. The dimensions are 9.1 cm x 7.9 cm x 3.2 mm thick. The G330 graphite was purified to impurities of less than 5 parts per million (5 PPM).

7.2 Experiment using Advanced Research Deposition System (ARDS) and Taylor Hobson Profilometer

After completing the ARDS chamber setup, the experiment was run in two steps with the first step being to deposit the CdTe at target thicknesses of: 1, 5, 10, and 15 µm. The second step was used to gather temperature data.

For the first part of the experiment, a predetermined substrate temperature of 250°C out of the position one heater was obtained. A temperature of 620°C on both the top and bottom heaters and time was varied at these temperatures. After five attempts of varying the time from 38 seconds to 31, 29, 25, and finally 20 seconds substrate

temperature of 252°C was achieved. After coming out of the position one heater, we then recorded temperature data at 60 second intervals for five minutes to measure the rate of the temperature drop. However, instead of the temperature dropping, it increased due to temperature of the structures nearby.

The CdTe films were deposited to achieve a target thickness of 1µm and 5µm respectively. For 1µm the deposition time was 55 seconds and for 5µm we ran 275 seconds.

It was determined to increase the substrate temperature to 350°C. The substrate temperature of 350°C was dialed in, the substrate was left in the heater for 60 seconds then came out at 359.8°C. After recording the substrate temperature data at 60 second intervals for five minutes, we found the temperature did indeed drop allowing us to continue with the experiment.

After running the experiment with the uncoated substrate, the 1 µm CdTe coated substrate and 5 µm CdTe coated substrate, all decreased in temperature tracking almost identically. It was then decided to increase the thickness of the CdTe to 10 µm and 15 µm and see what effect the thicker CdTe has on the temperature rate of decrease.

The 10 µm CdTe was deposited leaving the substrate in the CdTe deposition source for 650 seconds. The 15 µm CdTe was deposited leaving the substrate in the CdTe

deposition source for 975 seconds. The same experiment was run on the 10 μm and 15 μm CdTe substrates.

Taylor Hobson profilometer was then used to measure the CdTe film thicknesses on the four graphite substrates and check if the estimated values of thicknesses were indeed achieved.

The first graphite substrate coated with CdTe for 275 seconds was introduced into the measuring station and properly positioned on the work surface. Adjustments were made using the absolute position controller. The following conditions are made for our measurements.

1. Stylus tip radius = 5.0 μm
2. Measurement Speed = 0.5mm/s
3. Evaluation Length (trace length) = 10 mm
4. Data leveling: Best fit least squares line
5. No filtering
6. Step measurement: manual fit of cursors

The thickness was found to be 4.78 μm.

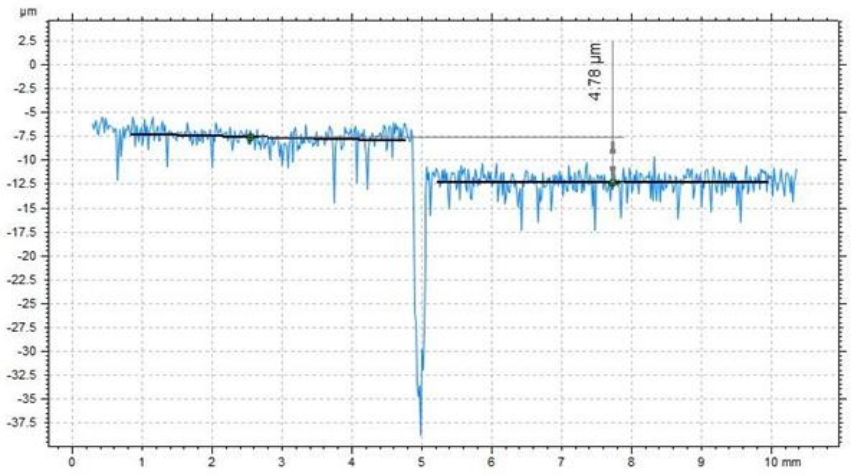

Figure 19: figure showing the thickness value calculated using DigiSurf software

Same procedure was adopted for other substrates also. The graphite substrates coated with CdTe for 55 seconds, 275 seconds, 650 seconds and 975 seconds were found to have thicknesses of 1 µm, 4.78 µm, 11.3 µm and 16.94 µm respectively.

7.3 Heat Transfer Calculations

These coated graphite substrates were then sent into the position one heater to collect the temperature data and the rate of cooling for coated graphite substrates was measured in comparison to the plain graphite and heat loss was calculated.

When we checked for the individual heat loss from the substrates, we found that the temperature was uniform and was not dropping towards the edge. There were no major temperature gradients in the middle, heat from the center is not going away through conduction. Hence Conduction heat loss was almost negligible.

The pressure during deposition and when the substrate was cooling down was 40 mTorr or 0.05 millibar, we calculated the convection heat loss as

Convection heat loss $q = h_c A dT$

Where

q = heat transferred per unit time (W)

A = heat transfer area of the surface (m^2) = $1m^2$

h_c= convective heat transfer coefficient of the process ($W/(m^2K)$ or $W/(m^{2o}C)$) = $2W/m^2$

dT = temperature difference between the surface and the bulk fluid (K or ^oC) = 100°C

q = 2*1*(100)

There was a Convection Heat Loss of 200 W/ m^2

Then we calculated the radiation heat loss

Radiation heat loss

$q = \sigma €T^4 A$

where

q = heat transfer per unit time (W)

€ = emissivity (0.8)

$\sigma = 5.6703\ 10^{-8}$ (W/m^2K^4) - The Stefan-Boltzmann Constant

T = absolute temperature Kelvin (K)

A = area of the emitting body (m^2), (Area is taken as $2m^2$ since there are two surfaces, top and bottom surfaces)

Calculating we have Radiation heat loss of $q = 6794W/m^2$

Hence, major heat loss was through Radiation.

CHAPTER 8: RESULTS

The substrate temperature of 350°C was dialed in and all the four CdTe coated graphite substrates along with the plain graphite substrate were individually left in the position heater one for 60 seconds. Then, after coming out of the heater, the substrates temperature data at 60 second intervals for five minutes was taken and compared to check the effect of CdTe on those substrates.

Table 4: table showing the results of rate of cooling for plain graphite substrate without CdTe

1st measurement		2nd Repetition		3rd Repetition		4th Repetition	
Time (Sec)	Temperature (°C)	Time (Sec)	Temperature (°C)	Time (Sec)	Temperature (°C)	Time (Sec)	Temperature (°C)
60	343.6	60	341.7	60	340.6	60	339
120	333	120	331.2	120	330.4	120	328.3
180	326.1	180	324.1	180	323.4	180	321.1
240	321.1	240	319	240	318.2	240	316
300	317.4	300	315.4	300	314.8	300	312.2

The Temperature vs Time graphs were plotted for all the four repetitions

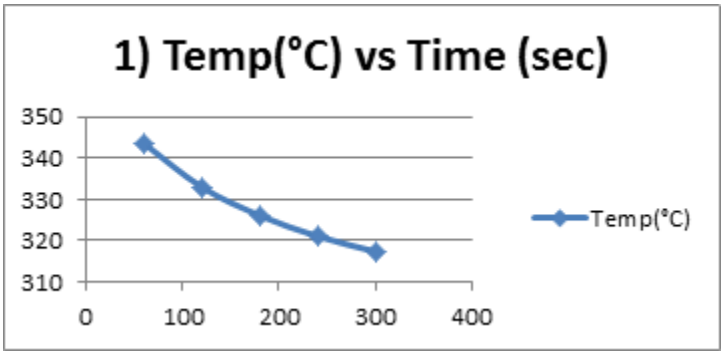

Figure 20: first measurement Temperature vs Time plot for plain graphite

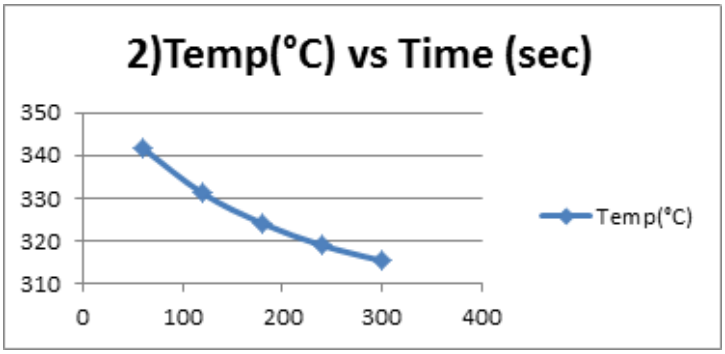

Figure 21: second repetition Temperature vs Time plot for plain graphite

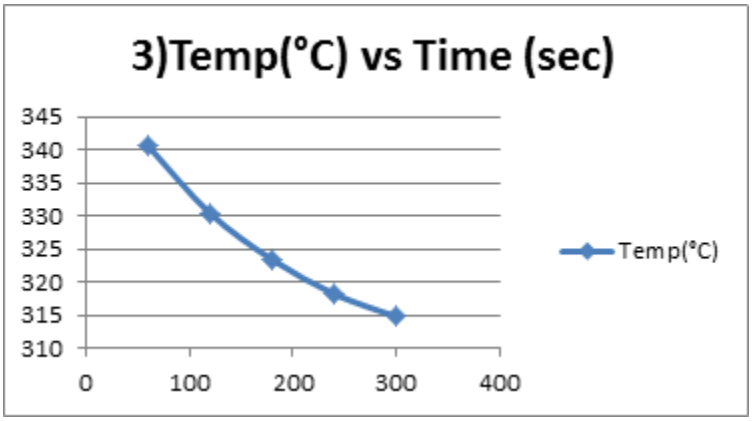

Figure 22: third repetition Temperature vs Time plot for plain graphite

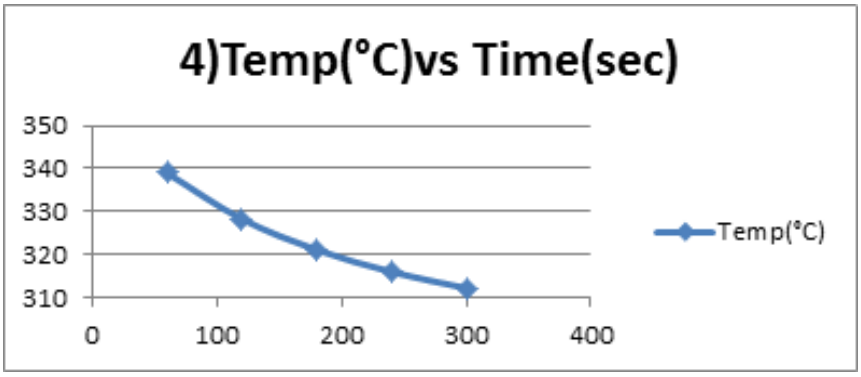

Figure 23: fourth repetition Temperature vs Time plot for plain graphite

Table 5: table showing the results of rate of cooling for graphite substrate coated with 1µm thick CdTe

1st measurement		2nd Repetition	
Time (sec)	Temperature (°C)	Time (sec)	Temperature (°C)
60	342	60	343.3
120	331.4	120	332.1
180	324.4	180	324.9
240	319.5	240	319.6
300	315.8	300	315.9

The Temperature vs Time graphs were plotted for both the repetitions

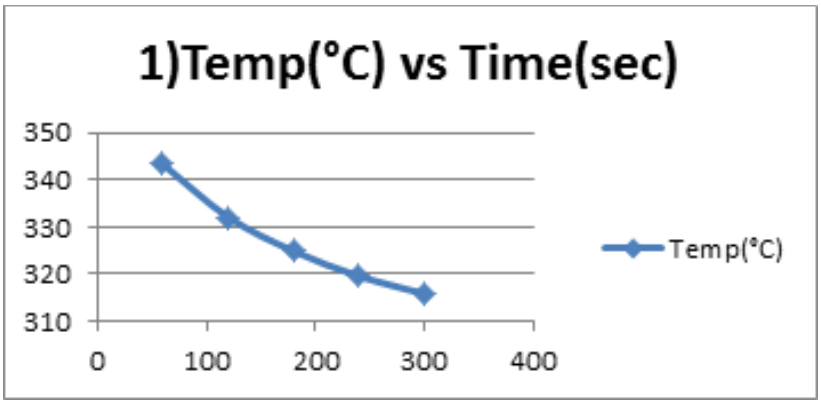

Figure 24: first measurement Temperature vs Time plot for graphite substrate with 1µm thick CdTe

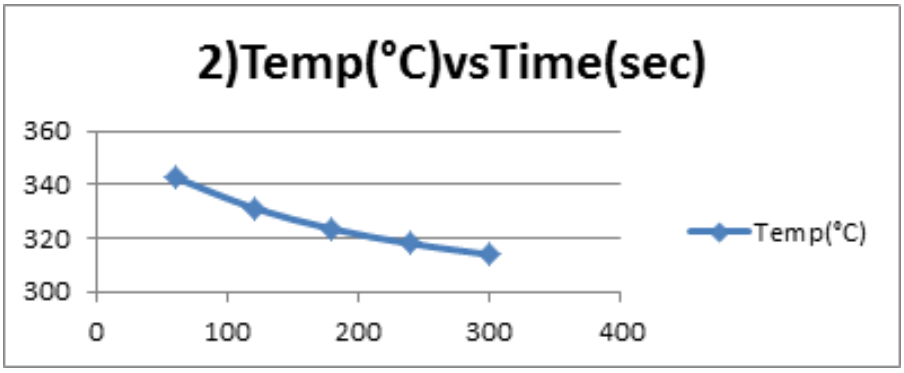

Figure 25: second repetition Temperature vs Time plot for graphite substrate with 1µm thick CdTe

Table 6: table showing the results of rate of cooling of graphite substrate coated with 4.78µm thick CdTe

1st measurement		2nd Repetition	
Time(sec)	Temperature(°C)	Time(sec)	Temperature(°C)
60	344.2	60	343.1
120	333.5	120	332.5

180	326.3	180	325.4
240	321.1	240	320.3
300	317.5	300	316.7

The Temperature vs Time graphs were plotted for both the repetitions

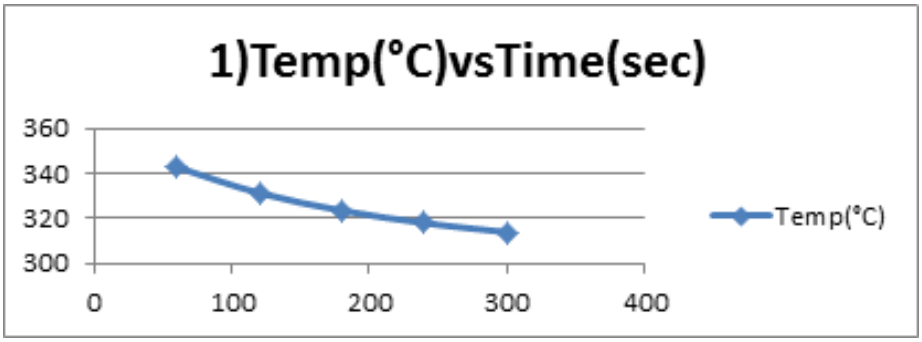

Figure 26: first measurement Temperature vs Time plot for graphite substrate with 4.78µm thick CdTe

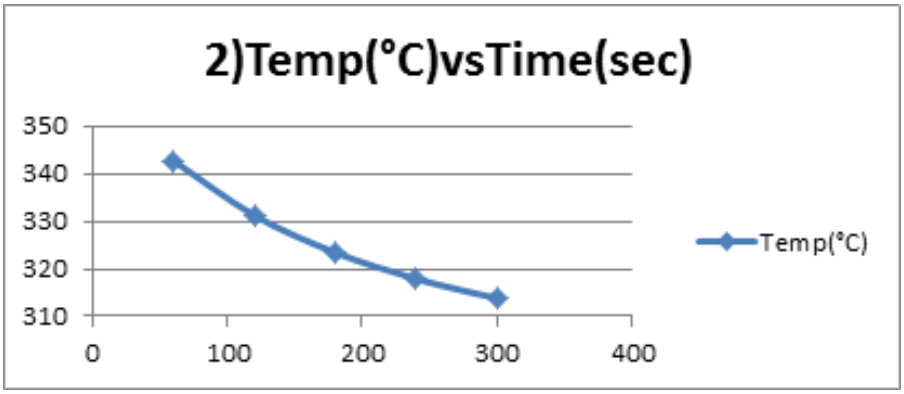

Figure 27: second repetition Temperature vs Time plot for graphite substrate with 4.78µm thick CdTe

Table 7: table showing the results of rate of cooling for graphite substrate coated with 11.3µm thick CdTe

1st measurement		2nd repetition	
Time (sec)	Temperature(°C)	Time (sec)	Temperature(°C)
60	342.9	60	340
120	331.5	120	329
180	323.8	180	321.6
240	318.2	240	316.2
300	314	300	312

The Temperature vs Time graphs were plotted for both the repetitions

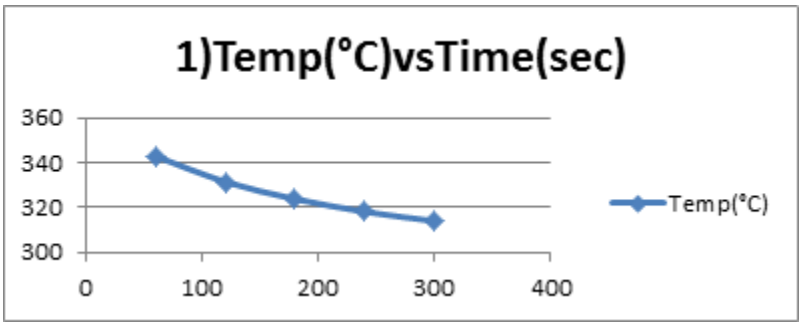

Figure 28: first measurement Temperature vs Time plot for graphite substrate with 11.3µm thick CdTe

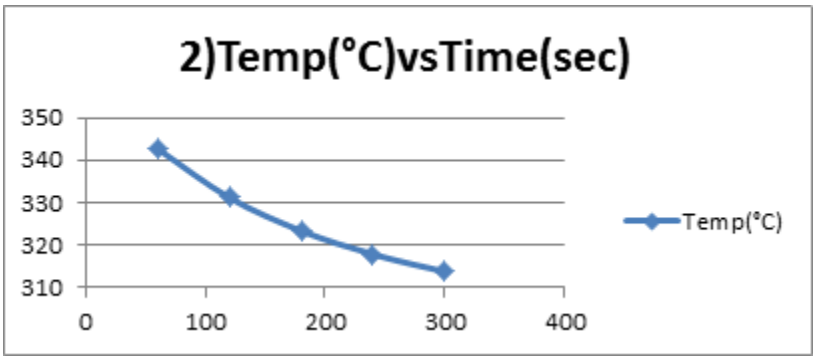

Figure 29: second repetition Temperature vs Time plot for graphite substrate with 11.3µm thick CdTe

Table 8: table showing the results of rate of cooling for graphite substrate coated with 16.94µm thick CdTe

1st measurement		2nd repetition	
Time(sec)	Temperature(°C)	Time(sec)	Temperature(°C)
60	343.3	60	342.7
120	331.8	120	331.2
180	324	180	323.4
240	318.2	240	317.9
300	314.2	300	313.8

The Temperature vs Time graphs were plotted for both the repetitions

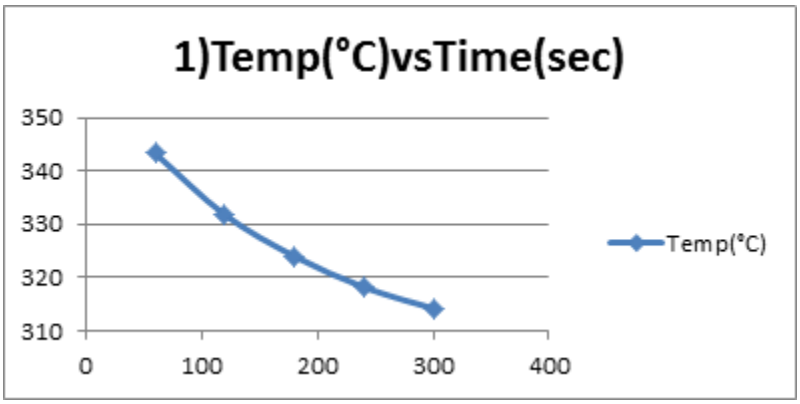

Figure 30: first measurement Temperature vs Time plot for graphite substrate with 16.94µm thick CdTe

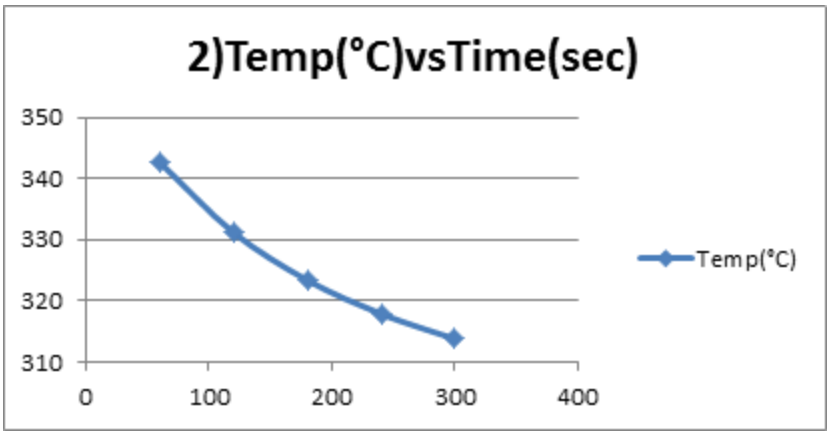

Figure 31: first measurement Temperature vs Time plot for graphite substrate with 16.94µm thick CdTe

As it can be observed, the temperature reached during heating and the rate of temperature during cooling was almost identical in all five substrates. Great care was taken to ensure all substrates were at ambient room temperature prior to starting the process and all temperatures were measured with the CdTe film facing down or away from the pyrometer. The collection of temperature data on the five substrates was repeated atleast two times each to ensure the accuracy and repeatability of the data. Since temperature drop is identical in all substrates we conclude that there is no change in the emissivity of graphite substrate when it is coated with CdTe. Here, the pyrometer generally sits at quite a distance from the substrate, it does not collect the radiation from different angles. The only radiation that is considered is the radiation that is coming out in normal direction. Hence, when we refer to the emissivity in our study, we mean only Perpendicular emissivity.

CHAPTER 9: CONCLUSIONS AND FUTURE WORK

9.1 Conclusions

The current work was an effort to investigate the effect on thermal performance on plain graphite and on graphite coated with variable thicknesses of CdTe inside the photovoltaic production tool. In this attempt the Kirchhoff's laws of radiation were studied and used in one part of the study. In another part, Angstrom sun technologies Thin film Probe software was used to simulate a CdTe-graphite layer stack. In the final part, the equipment of ARDS and Taylor Hobson Profilometer was used to deposit and measure the film thickness.

Refractive indices of CdTe, graphite and Air from published literature and Fresnel's equation were used to calculate the emissivity of graphite coated with CdTe. From the results it was found that CdTe did not have an effect on graphite as the emissivity value for the stack remained almost unchanged.

Then, in the effective wavelength range, a CdTe-graphite layer stack was simulated. The reflection values of graphite coated with different thicknesses of CdTe were deduced and used in calculating the emissivity. All the layer stack results showed negligible effect of CdTe on graphite substrate.

In the final part, we used Advanced Research Deposition system to coat CdTe on graphite substrates and measured the individual thicknesses using Taylor Hobson

profilometer. Then, the rate of cooling for coated graphite substrates was measured in comparison to the plain graphite.

Four set of repetitions for the rate of cooling for coated graphite substrates was measured in comparison to the plain graphite and tried to evaluate the effect of CdTe on them. Repetitions were made to ensure the data is consistent. We found that the temperature drops were identical and there was no major effect of CdTe on the graphite substrates.

Experimental verification was needed because primary evaluation using Kirchhoff's laws and simulation software tool were conducted basing on the approximate values from the literature. Finally, Considering the results in all the three parts, we can conclusively say that there is a negligible effect on the thermal performance on plain graphite and graphite coated with variable thicknesses of CdTe inside the production tool.

9.2 Future study

In the manufacturing of CdTe solar cells, CdS, $CdCl_2$ are also used. An understanding of the emissivity of graphite coated with these materials is needed.

REFERENCES

1) http://www.firstsolar.com/en/technologies-and-capabilities/pv-modules/first-solar-series-3-black-module/cdte-technology

2)http://www.firstsolar.com/Our-Solutions

3) Lazard's Levelized Cost of Energy Analysis-Version 8.0, , published September 2014, Available http://www.lazard.com/PDF/Levelized%20Cost%20of%20Energy%20-%20Version%208.0.pdf, accessed October 2014

4) Jason Kephart et. al;, published in Progress in Photovoltaics (2015)

5) V. M. Fthenakis and H. C. Kim, CdTe Photovoltaics: Life Cycle Environmental Profile and Comparisons, Thin Solid Films, 515 (2007), 5961-5963

6) Statement by CEO of First Solar at the 2007 Solar Power Conference

7) J. T. Mullins, J. Carles and A. W. Brinkman. "High Temperature Optical Properties of Cadmium Telluride ". J. Appl. Phys., 81 (1997) 6374

8) D C Rodway et al*.,* 1983. In situ AES and work-function study of the deposition of caesium on CdTe. Journal of Physics, D: Appl. Phys. 16 2317*,* 1983

9) Zhenjie Chen et al., Preparation and Characterization of Optically Active Polyacetylene@CdTe Quantum Dots Composites with Low Infrared Emissivity. Journal of Inorganic and Organometallic Polymers and Materials May 2014, Volume 24, Issue 3, pp 591-599

10) I. Avetissov et al., Modeling of axial vibrational control technique for CdTe VGF crystal growth under controlled cadmium partial pressure. Volume 385, 1 January 2014, Pages 88–94

11) J.A. Reizes, Transport Phenomena in Heat and Mass Transfer. Elsevier- publisher

12) G. W. AUTIO and E. SCALA. Normal spectral emissivity of isotropic and anisotropic materials, AIAA Journal, Vol.3, No. 4 (1965), pp. 738-740

13) Dost & Lent, Single Crystal Growth of Semiconductors from Metallic Solutions. Elsevier Science

14) http://www.altenergy.org/renewables/solar.html

15) http://www.solar-facts-and-advice.com/cadmium-telluride.html

16) A. J. Strauss. "The Physical Properties of Cadmium Telluride". Appl. Phys. Rev., 12 (1977)167

17) Refractive index of CdTe (Cadmium telluride) - DeBell-300K http://refractiveindex.info/?shelf=main&book=CdTe&page=DeBell-300K

18) http://www.raytek.com/Raytek/en-r0/IREducation/EmissivityNonMetals.htm